Photovoltaic performance of quasi-solid state dye sensitized solar cells based on perylene dye and modified TiO$_2$ photo-electrode

P. Balraju [a], Manish Kumar [b], Y.S. Deol [b], M.S. Roy [b], G.D. Sharma [a,c,*]

[a] Molecular Electronic and Optoelectronic Device Laboratory, Department of Physics, JNV University, Jodhpur, Rajasthan 342005, India
[b] Defence Laboratory, Jodhpur, Rajasthan, India
[c] Jaipur Engineering College, Jaipur, Rajasthan, India

ABSTRACT

The influence of compact layer of TiO$_2$ between FTO and nano-porous TiO$_2$ on the charge transport and photovoltaic properties of quasi-solid state dye sensitized solar cells with polymer gel electrolyte and perylene derivative dye as sensitizer was investigated. The PEDOT:PSS/graphite/FTO was used as counter electrodes for present investigation. The modification of photo-electrode significantly improve the power conversion efficiency (2.94%) of the solar cells attributed to the higher electron lifetime and reduction in recombination processes as indicated by the electro-chemical impedance spectra of the solar cell. The compact layer provide a large TiO$_2$/FTO contact area, reduce the electron recombination by blocking the direct contact with the redox couple in the electrolyte and efficient collection of electrons by FTO electrode. Finally, the incorporation of TiO$_2$ nano-particle in the polymer electrolyte further improves the power conversion efficiency (3.2%) of the device attributed to the improved ion transport.

© 2009 Elsevier B.V. All rights reserved.

1. Introduction

In recent years, there has been growing interest in organic based solar cells to replace the conventional inorganic solar cells due to their low cost and low temperature processing [1–10]. Among them dye sensitized solar cells have attracted much attention because of their comparable power conversion efficiency with conventional inorganic photovoltaic devices at relatively low cost. Since the discovery of DSSCs in 1991s [11], these devices have been regarded as promising next generation photovoltaic devices because of their unique characteristics such as transparency and various colors as well as low cost. The DSSCs are composed of a dye-adsorbed wide band gap nano-crystalline oxide film on transparent conducting substrate used as photo-electrode, a redox electrolyte and a metallic counter electrode. The dye molecules play an important role in generating photo-excited electrons, the wide band gap nano-crystalline film provides a pathway for photo-excited electrons to move from dye to transparent conducting substrate and the redox electrolyte delivers electrons from counter electrode to oxidized dye to regenerate dye. The photovoltaic performance of these devices influenced by many factors such as morphology, film structure, porosity and particle size of the nano-crystalline semiconductor used as photo-electrode, molar absorption coefficient,

absorption wavelength of photo-sensitizer dye, type of electrolytes, solid–solid and/or solid–liquid interfaces and electron transportation and recombination rates occurring in the device.

The improvement in the solar cell performance has been achieved by extensive studies on the optimization of dye, semiconductor film and redox electrolyte [12–16]. The DSSCs based on ruthenium dye sensitized nano-crystalline TiO$_2$ electrodes and liquid redox electrolytes have already reached power conversion efficiency in the range 9–11% [17,18]. However, in view of high cost and environmental issues related to ruthenium dye will limit the large scale application of DSSCs. Metal free organic dyes, which have many advantages such as large absorption coefficient, easy molecular design for desired photophysical and photochemical properties, are also adopted as sensitizers for DSSCs and recently, the highest over all conversion efficiency of DSSCs based on these organic dye has reached a considerable level of 9%, indicating that these would be a promising type of sensitizers for DSSCs [19–25].

The main problems caused by the liquid electrolytes such as such as the leakage and volatilization of liquid, are the critical factors that limits the long-term performance and practical use of the DSSCs. Thus, many efforts have been made to replace the liquid electrolyte with solid or quasi-solid-type charge transport materials such as polymer gel electrolytes [26–28] and solid polymer electrolytes [29–31] to overcome above critical factors.

To improve the power conversion efficiency of the DSSCs, a unidirectional charge flow in the device is essential. According to the unidirectional electron transporting principle of DSSCs, there are four important interfaces, such as FTO/TiO$_2$, TiO$_2$/dye,

dye/electrolyte and electrolyte/counter electrode. Recently many researchers have paid much attention to modify the interface of FTO/TiO_2 [32–35]. It has been reported that the back transfer of electrons to the electrolyte from FTO substrate can be prevented, when the TiO_2 thin layer is coated directly on to the FTO glass substrate through spray pyrolysis technique [36–38], sputtering method [39,40] and chemical vapor deposition method [41].

Counter electrode with high electro-chemical activity is also an important requirement of an efficient DSSCs. Usually, a transparent conducting oxide (TCO) substrate coated with platinum (Pt) is being used as a counter electrode in DSSCs. Pt electrode shows superior electro-chemical activity, but it is highly expensive for the fabrication of low cost DSSCs. As a counter electrode PEDOT doped with polystyrene sulphonated (PSS) (PEDOT:PSS) [42–44] has been studied in liquid and gel electrolyte assemblies.

We are particularly interested in dyes based perylene derivatives owing to their unique outstanding chemical, thermal and unique photochemical stabilities [45–47] and have been investigated as sensitizers for DSSCs [48,49]. In the present investigation, an effort have been made to prepare a low cost quasi-solid state dye sensitized solar cell with sputter deposited TiO_2 photo-electrodes, PEDOT:PSS/graphite coated FTO counter electrode, perylene derivative dye as sensitizer and a quasi-solid state polymer electrolyte with and without containing TiO_2 nano-particles as nano-filler. The optical properties of the resulting TiO_2 photo-electrodes and photovoltaic properties of the quasi-solid state dye sensitized solar cells have been investigated. The electro-chemical impedance spectroscopy measurement was used to examine the kinetic processes in quasi-solid state DSSCs.

2. Experimental detail

2.1. Synthesis of perylene-3,4,9,10-teracarboxylic acid (PTCA)

Perylene-3,4,9,10-tetracarboxylic acid (PTCA) was obtained according to literature [50]. 3,4.9,10-Perylenetetracarboxylate was prepared by dissolution of 3,4, 9,10-perylenetetracarboxylic dianhydride (Aldrich) (1 mmol) into a dilute solution of KOH. Then, 1 M HCl was added dropwise until a precipitate formed, which was collected, kept from heat, and vacuum dried at room temperature to yield red powder of perylene-3,4,9,10-tetracarboxylic acid (PTCA). The molecular structure of the PTCA is shown in Fig. 1.

Cyclic voltammetry (CV) of the dye and dye sensitized TiO_2 was performed using a potentiostat–galvanostat (PGSTAT 30, Autolab, Eco-Chemie, Netherlands) in a three-electrode cell at room temperature. The three-electrode cell was comprised of a gold working electrode, a platinum counter electrode and an SCE reference electrode, calibrated against the Fc/Fc^+ couple (+0.470 V vs. SCE). It was conducted in a distilled N,N-dimethylformamide (DMF) solution containing 10^{-3} M of the dye and 0.1 M KCl as supporting electrolyte at a scan rate of 60 mV/s. The highest occupied molecular orbital and lowest unoccupied molecular orbital energy levels were estimated from these measurements are 6.01 and 4.0 eV, respectively, which are same as reported earlier [51]. The optical absorption spectrum of the materials used for present investigation was recorded on PerkinElmer UV–vis spectrophotometer.
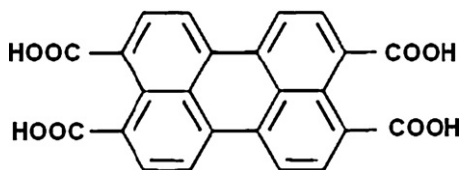

Fig. 1. Perylene-3,4,9,10-tetracarboxylic acid (PTCA).

2.2. Preparation of dye sensitized TiO_2 coated FTO electrode

The conducting glass substrate (fluorine doped tin oxide) (FTO) was cleaned and rinsed with water and 2-propanol, then, soaked in 2-propanol for 12 h. The FTO substrate was dried in vacuum prior to film preparation. The TiO_2 colloidal solution was prepared by grinding in a mortar with pestle 6 g of TiO_2 (P25 Degussa) powder in 2 ml of distilled was water and 0.2 ml of acetylacetone, the substances were ground for 40 min. Finally 8.0 ml of distilled water and 0.1 ml of Triton X-100 were slowly added with continuous mixing for 10 min. The finely grinded paste was coated over florine doped tin oxide (FTO) glass by doctor blade technique and dried at room temperature. The thickness of the porous layer of was controlled by an adhesive tape. Thereafter, the film was sintered at 450 °C for 30 min in ambient condition. After sintering, the film was cooled to room temperature and the TiO_2 film shows good adhesion with FTO surface. The thickness of the obtained porous TiO_2 film was approximately 5–10 μm.

Dye sensitization was carried out by soaking the nano-porous TiO_2 film in 5×10^{-4} M solution of PTCA, in ethanol for more than 12 h at room temperature and, then rinsed. After the sensitization, a quasi-solid state polymer electrolyte containing 0.038 g of P25 TiO_2 powder, 0.5 M KI/0.05 I_2, 0.26 g of PEO and 44 μl of 4-tert-butylpyridine in 1:1 acetone/propylene carbonate was spread on the dye sensitized TiO_2 film by spin coating to form a hole conducting layer.

Counter electrode was made by developing a thin film of PEDOT:PSS over graphite coated FTO glass substrate. In this process, first the FTO is coated with graphite and then DMSO treated PEDOT:PSS was grown over the top of the film by dip coating method. The film was treated dried at 80 °C for 30 min. Finally both electrodes were clamped together to form a layered structure of quasi-solid state dye sensitized solar cell. We have fabricated following devices:

(D1) FTO/np-TiO_2/dye/polymer electrolyte/PEDOT:PSS/graphite/ FTO.
(D2) FTO/compact TiO_2 layer/np-TiO_2/dye/polymer electrolyte/PEDOT:PSS/graphite/FTO.
(D3) FTO/compact TiO_2 layer/np-TiO_2/dye/polymer electrolyte with np-TiO_2/PEDOT:PSS/graphite/FTO.

The structure of the quasi-solid state DSSC with compact layer in the photo-electrode and polymer electrolyte is shown in Fig. 2. The electro-chemical impedance spectra (EIS) measurements were carried out by applying bias of the open circuit voltage (V_{oc}) and recorded over a frequency range 1 mHz to 10^5 Hz with ac amplitude of 10 mV with an electro-chemical analyzer equipped with FRA. The current–voltage (J–V) characteristics in dark and under illumination intensity of 100 mW/cm² were measured with Keithley electrometer having built in power supply. A 100 W halogen lamp was used as light source

3. Results and discussion

3.1. Optical properties

Fig. 3 shows the optical absorption spectra of TiO_2, PTCA and PTCA dye sensitized TiO_2 photo-electrode. The optical band gap (E_{gopt}) of PTCA estimated from the band edge of absorption (~620 nm) was 2.01 eV. As can be seen from Fig. 3 that when the PTCA was adsorbed on TiO_2, the absorption peak was broaden and slightly shifted to longer wavelength. The carboxylate group of C–O–Ti served as an interlocking group which enhanced the electric coupling between π^* orbital of the perylene and Ti(3d) orbital
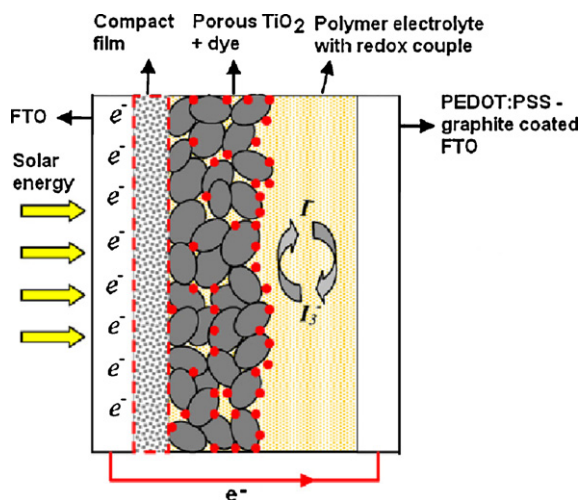
Fig. 2. Schematic diagram of quasi-solid state DSSC with compact TiO₂ layer, porous TiO₂ + dye, polymer electrode with redox couple and PEDOT:PSS-graphite coated FTO counter electrode.

Fig. 5. Optical absorption spectra of the PTCA dye sensitized TiO₂ sensitized photo-electrode (a) without compact layer and (b) with compact layer.

at 1713 cm^{-1} attributed to the stretch band of carboxyl (COOH) group and the peak at 1400 cm^{-1} results from the plane bending of C–O–H. After the PTCA was adsorbed into TiO₂ surface, the peaks attributed COOH at 1713 cm^{-1} and peak at 1400 cm^{-1} due to the plane bending of C–O–H, disappeared, while a symmetric peak at 1420 cm^{-1} for COO$^-$ group was observed. This observation shows that the deprotonation of –COOH group is taking place on the TiO₂ surface, indicating a bidentate chelating mode for the anchoring of the PTCA on the TiO₂ surface. Other main vibration bands located at 1504 cm^{-1} for C–C stretching, 1367 cm^{-1} for C–H bending were not influenced after the PTCA adsorption onto the TiO₂ surface.

The effect of dye adsorption on the TiO₂ electrode was investigated by absorption measurements in the wavelength range 360–740 nm. Fig. 5 illustrate the absorption spectra of the dye sensitized photo-electrode with and without TiO₂ compact layer. It was observed that there is slight change in the absorption spectra of dye sensitized TiO₂ photo-electrode with and without compact TiO₂ layer in wavelength range 440–640 nm. The intensity of absorbance is slightly more in the photo-electrode with compact layer for whole range. The slight change in the spectrum may due to a slightly different dye adsorption time or different extension of the surface of the porous TiO₂ layer.
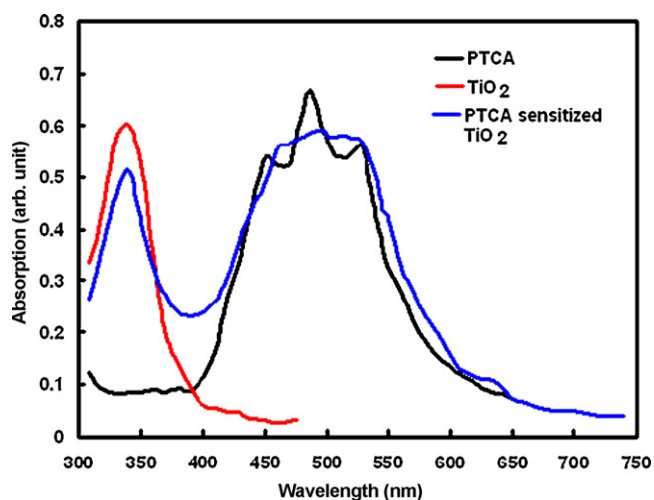

Fig. 3. Optical absorption spectra of PTCA TiO₂ nano-porous film and PTCA sensitized TiO₂ films.

manifold of the semiconductor. Thus it would increase the delocalization of the π* orbital of perylene, which result in the red shift of the absorption spectra [52].

The binding mode of the PTCA molecules to the TiO₂ surface, which is associated with the interfacial electron injection, was analyzed by the FTIR technique. Fig. 4 shows the FTIR spectra of PTCA power and PTCA sensitized TiO₂ film. For PTCA, the peak appeared
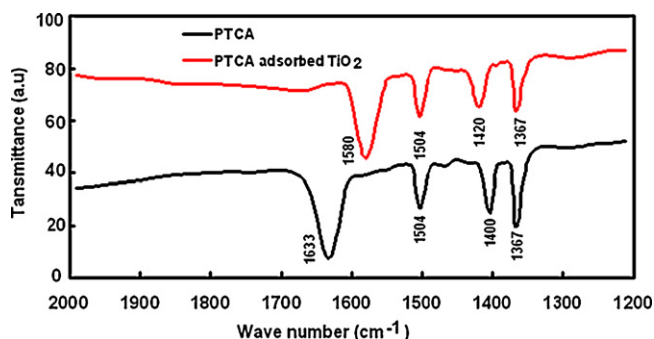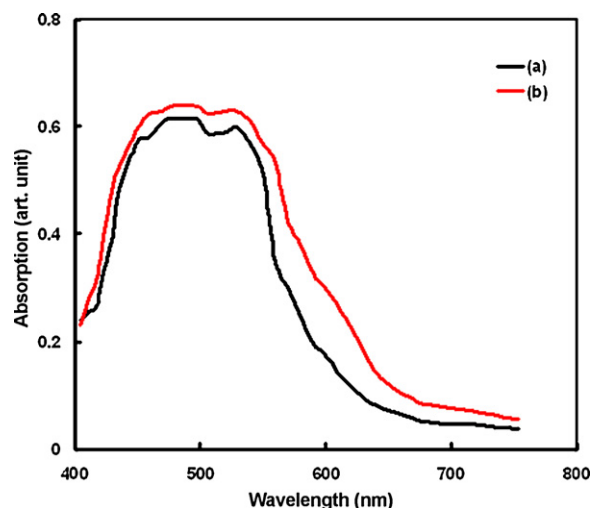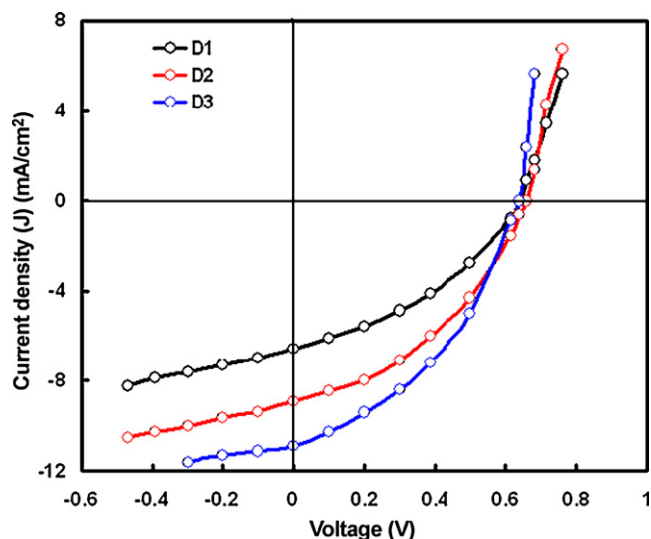
3.2. Photovoltaic properties

The current–voltage characteristics of the DSSCs (D1 and D2) based on different photo-electrodes under illumination are illustrated in Fig. 6 at the illumination intensity of 100 mW/cm^2 and the photovoltaic parameters are summarized in Table 1. Fig. 7 shows the IPCE spectra of the quasi-solid state DSSCs. The IPCE spectra of both DSSCs follows the absorption spectra of PTCA sensitized photo-electrodes. This indicates that the photo-electrodes are the photoactive layers of the solar cells. As can be seen from Fig. 7 that the IPCE is higher for the DSSC D2 than that for D1. The IPCE of the DSSC can be expressed in terms of the light harvesting efficiency (LHE), the quantum yield of the charge injection (ϕ_{inj}), and the efficiency (η_c) of collecting the injected charge at back contact as shown in following expression:

$$IPCE = LHE(\lambda)\phi_{inj}\eta_c$$

The LHE (λ), is mainly proportional to the adsorbed dye molecules per square centimeter, ϕ_{inj} and η_c are related to the crystallinity of the TiO₂ nano-particles. The η_c depends upon the film resistance and the electron lifetime (τ_n).

Fig. 4. FTIR spectra of PTCA (powder) and PTCA adsorbed TiO₂ film.

Table 1

Performance comparison of the quasi-solid state DSSCs employing with and without compact TiO_2 layer in photo-electrode at illumination intensity $100\,mW/cm^2$.

Photo-electrode	Short circuit photocurrent (J_{sc}) (mA/cm^2)	Open circuit voltage (V_{oc}) (V)	Fill factor	Power conversion efficiency (η) (%)
Without compact layer	7.4	0.64	0.43	2.03
With compact layer	9.3	0.66	0.48	2.94

Fig. 6. Current–voltage characteristics of D1, D2 and D3 quasi-solid state DSSCs under illumination.
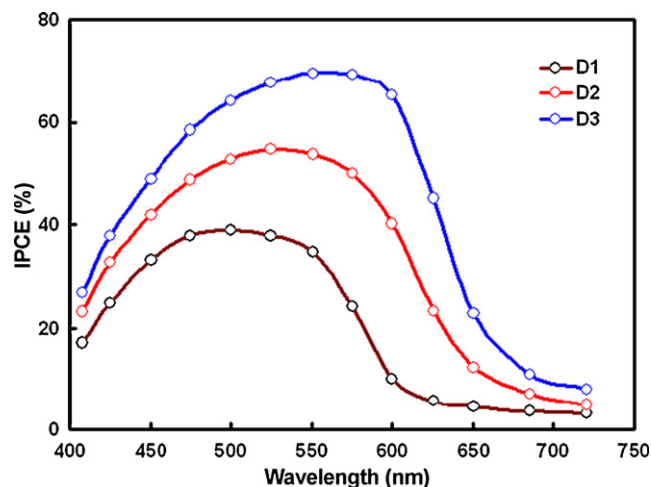
In order to identify the mechanism of the IPCE enhancement in D2, the dye loading on the TiO_2 surface of both electrodes was investigated. The adsorbed dye of TiO_2 surface on both electrodes was first eluted completely in the NaOH solution then subjected to the qualitative analysis using UV–vis spectroscopy. We found that the number of dye molecules absorbed on the surface of photo-electrode with compact layer is almost same for both photo-electrodes (slightly higher for photo-electrode with compact layer). Therefore, the enhancement in IPCE is not due the dye absorbed in the photo-electrode. We assume that the LHE and ϕ_{inj} played a minor role in the enhancement in IPCE and the dominating factor may be the increased electron collection efficiency (η_c). The increased value of η_c, may be due to the increased number of electron pathways to the compact layer and blocking effect of back electron transfer to the electrolyte. The former mechanism originates from the dense structure of the compact layer. Under

a constant illumination intensity and amount dye adsorbed, the number of photogenerated electrons is almost same for both DSSCs. Therefore, η_c and recombination rate will determine the IPCE. An increased contact area of compact TiO_2 layer with FTO surface and decrease in electron transfer resistance leads to an increase in the η_c. At the same time, the compact layer also reduces the reaction sites, which are responsible for the back electron transfer, leading to suppression of back electron transfer. The combination of above factors together, leads to the improvement in η_c, results an enhancement in IPCE.

The DSSC D2 shows high short circuit photocurrent (J_{sc}) than DSSC D1. The short circuit photocurrent of DSSC is mainly influenced by two factors: dye loading and charge recombination at photo-electrode [53,54]. Since the amount of dye loading is almost same in both photo-electrodes, suggesting that the amount of dye loading has little effect on the J_{sc}. Therefore, the main factor influencing the J_{sc} of the DSSCs may be the charge recombination at FTO/electrolyte interface. When a compact layer TiO_2 is inserted between FTO and nano-porous TiO_2 film, the recombination sites are reduced and charge recombination in the DSSC is effectively suppressed as demonstrated by the dark current (dark current is smaller for DSSC D2). The increase in J_{sc} is generally related to the enhancement of the number of photogenerated electrons, which are efficiently transferred to TiO_2 electrode. The enhancement of J_{sc} with compact layer may be due to following reasons: (i) the compact layer act as seeding layer, which modify the microstructure of the upper TiO_2 thin films, that in turn induces the different dye absorption, (ii) results the increase in the protection effect against the ionic penetration from the electrolyte through the blocking layer, and (iii) the TiO_2 blocking layer has both rutile and anatase phase having band gap between 3.0 and 3.2 eV and upper nano-porous sol gel TiO_2 film has only anatase phase having band gap 3.2 eV. Therefore, the injected excited electrons moves in the direction lower than energy conduction band from the porous TiO_2 to the blocking TiO_2 layer, thus resulting smooth electron movement as shown in Fig. 8. Since the dye adsorption by both the electrodes is almost same, we conclude that the enhancement in the J_{sc} is only due to the (ii) and (iii) reasons.

The fill factor for DSSC D2 is higher than that for D2. The resistance of TiO_2 photo-electrode contributes to total series resistance of the solar cell. The DSSC D1 has only nano-porous TiO_2 photo-electrode, which increase over all series resistance of solar cell, which in turns decrease the fill factor. Additionally, the density of compact layer is higher than that of porous structure of nano-porous TiO_2. As a result, more effective electron pathways are generated via this compact layer to facilitate electron transfer. Consequently, more electrons can be collected at the conduction band of the photo-electrodes and transferred to external circuit, results an improvement in J_{sc} of the DSSC D2.

The open circuit photovoltage decay (OCPVD) technique has been employed to get information about the electron lifetime and also provide some quantitative information about information about electron recombination in DSSC [55]. In order to conduct the OCPVD measurement, the DSSC was illuminated by light, steady state voltage was obtained, and subsequent decay of V_{oc} after stopping the illumination was monitored under open circuit condition [56]. The decay of the photovoltage reflects the decrease of the electron concentration at the FTO surface, which is mainly caused by the charge recombination. Fig. 9 shows the OCPVD decay curves of

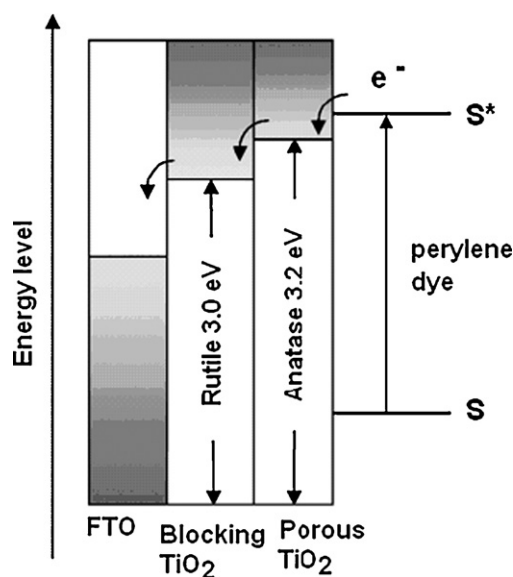**Fig. 7.** IPCE spectra of quasi-solid state DSSCs D1, D2 and D3.

Fig. 8. Energy band diagram of blocking TiO$_2$ layer/nano-porous TiO$_2$/dye photo-electrode.

Fig. 10. Variation of short circuit photocurrent (J_{sc}) with illumination intensity (P_{in}).

quasi-solid state DSSCs D1 and D2. It was observed that the OCPVD response of the D2 was slower than that D1. From the OCPV experiment, the electron lifetime (τ_n) is derived by fitting an exponential function of the photovoltage decay to $\exp(-t/\tau_n)$. The lifetime calculated from the exponential fit of the decay are found to be 34 and 21 ms for the D2 and D1, respectively. The electron lifetime (τ_n) control the extent of electron recombination with the redox electrolyte couple. Since the dye adsorption due to the introduction of compact layer is negligible, the difference in the OCPVD was mainly due to the blocking effect of the compact layer. This suggested that the electrons injected from excited dye could survive for longer time hence can facilitate the electron transport without the undergoing losses at the FTO surface. Therefore, the compact layer is able to reduce the photo-electron recombination.

Since the amount of the photogenerated electrons is directly related to the illumination intensity (P_{in}) of light, the dependence of J_{sc} with the P_{in} also provide the useful information about the electron kinetics due the introduction of compact layer in the quasi-solid state DSSC. Fig. 10 shows that the J_{sc} of the D1 and D2 follow
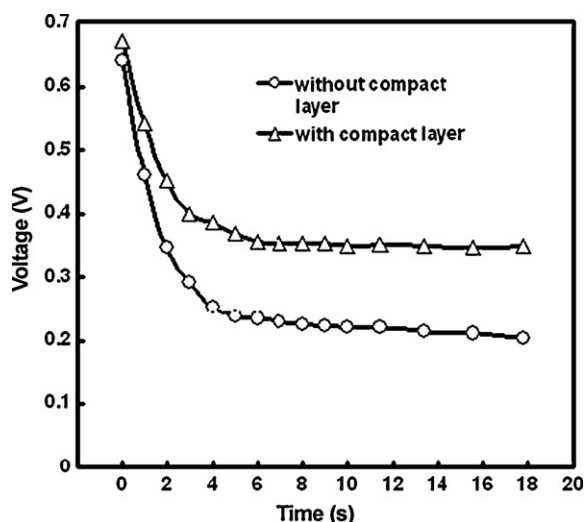
the power law dependence with P_{in} with different exponent, i.e. 0.29 and 0.24, respectively. The value of exponent for D2 with compact layer is 21% higher for than that for D1, indicates that 21% more electrons are collected from the same amount of photogenerated electron at the FTO surface.

3.3. Electro-chemical impedance spectroscopy

Electro-chemical impedance spectroscopy (EIS) has proven to be useful technique for the characteristics of electronic and ionic processes in DSSCs [57,58]. Fig. 11(a) shows Nyquist plots of quasi-solid state DSSCs. Three typical semicircles in the Nyquist plots

Fig. 11. (a) Nyquist plots of EIS spectra of quasi-solid state DSSCs made fro different photo-electrodes. (b) Bode plots of impedance of quasi-solid state DSSCs employing different photo-electrodes.

Fig. 9. Open circuits photo voltage decay curves of the quasi-solid state DSSCs with and without compact layer in photo-electrode.

Table 2
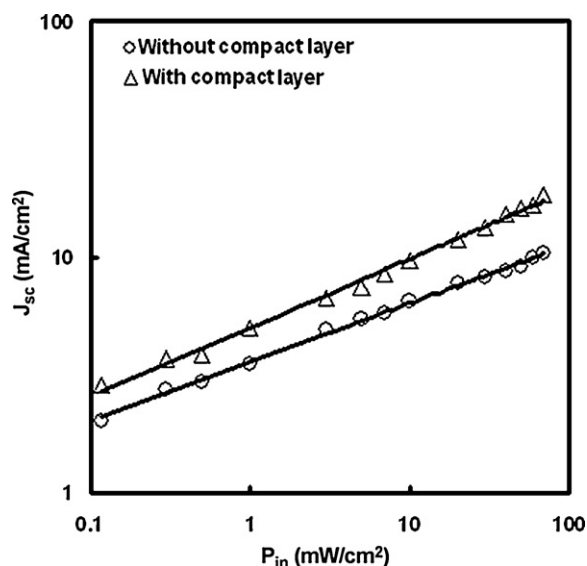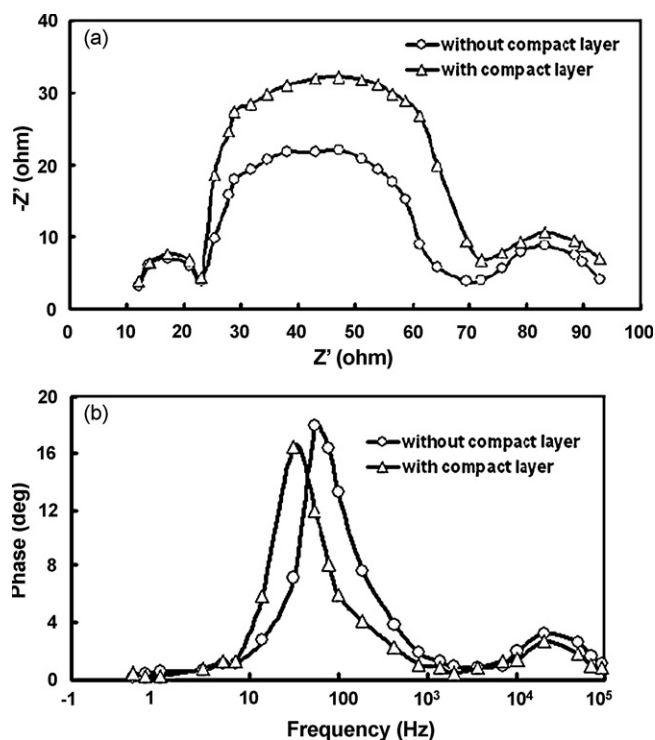The values of kinetic parameters within the photo-electrodes employed for quasi-solid state dye sensitized solar cells.

Photo-electrode	Charge transport resistance (R_{ct}) (Ω)	Transport resistance (R_w) (Ω)	Electron lifetime (τ_n)
Without compact layer	43.5	26.6	23 ms
With compact layer	39.4	24.7	34 ms

were observed, which corresponds to the I_3^- transport in the electrolyte (low frequency semicircle), electron recombination at the TiO_2/electrolyte interface together with the electron transport in the TiO_2 network (middle frequency semicircle) and charge transport process at the interface between redox couple and counter electrode (high frequency semicircle) in order of increasing frequency [55–63]. The identical semicircles for both D1 and D2 in high frequency region indicates that the compact TiO_2 layer do not have any impact the charge transfer at counter electrode/electrolyte. It is interesting that the semicircle corresponding to TiO_2/dye/electrolyte interface gets larger for the DSSC D2 than that for D1. At open circuit, the electrons which are injected from the adsorbed dye to the TiO_2 nano-particles partially accumulate at the interface of the TiO_2/dye/electrolyte and react with electrolyte, thereby decreasing the impedance of the this network. Therefore, the larger semicircle of the DSSC (D2) shows that the recombination of photogenerated electrons with the electrolyte by the backward transfer is retarded by using modified photo-electrode. Fig. 11(b) shows the Bode phase plots of EIS spectra for the DSSC, made with different photo-electrodes. Two peaks associated with the transfer of the photogenerated electrons at the surface of TiO_2 nano-particles and the conducting electrodes, are clearly observed. The frequency peak at the high frequency region can be ascribed to the charge transfer at the interfaces of the electrolyte/counter electrode, and the other low frequency region to the accumulation/transport of the injected electrons with TiO_2 porous film and the charge transfer at the interfaces of electrolyte, respectively.

The middle frequency semicircles in Fig. 11(a) can be fitted with a charge transport resistance (R_{ct}), which is shunt wound with a constant phase element (CPE) and both of them are connected in series with a transport resistance (R_w) on injected electrons within the TiO_2 film. According to the EIS model developed by Kern [64], the lifetime (τ_n) of injected electrons in TiO_2 film can be estimated from the position of the low frequency peak in Fig. 10(b), through the expression $\tau_n = 1/2(\pi f)$, where f is the frequency of superimposed ac voltage. The fitted values of R_{ct}, R_w and τ_n for the quasi-solid state DSSC made for different photo-electrodes are shown in Table 2. The lower value of R_w and higher value of electron lifetime for the quasi-solid state DSSC D2 result an enhancement in power conversion efficiency as compared to the DSSC D1.

3.4. Effect of np-TiO_2 nano-fillers in the polymer electrolyte

We have investigated the effect on TiO_2 nano-particles incorporation in polymer electrolyte on charge transport and photovoltaic response in quasi-solid state DSSC (D3) having structure FTO/compact TiO_2 layer/np-TiO_2/dye/counter electrode. The current–voltage (J–V) characteristics of the device under illumination of the device D3 is also shown in Fig. 6. It is observed that the short circuit current (J_{sc}) (10.9 mA/cm^2) is significantly enhanced by the incorporation of TiO_2 nano-particles in the polymer electrolyte, and slight decrease in open circuit voltage (V_{oc}). The J–V characteristics of D2 and D3 quasi-solid state DSSCs, in dark are shown in Fig. 12. This shows that nano-fillers in polymer electrolyte, causes a reduction in dark current and attributed to the lower concentration of free tri-iodide ions near the dye attached TiO_2 surface because the surfaces of the nano-filler can immobilize the ions. This also results slightly smaller V_{oc} due to the high electron concentration at TiO_2 surface of electrolyte. The charge
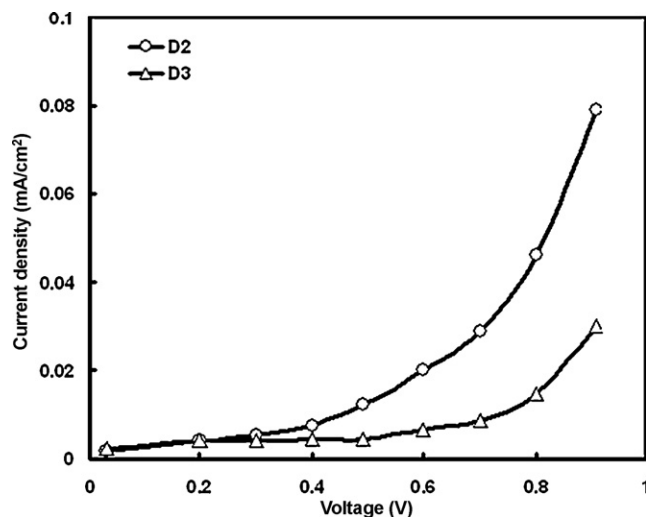

Fig. 12. Current–voltage characteristics of quasi solid state DSSC in dark based on different polymer electrolytes.

transport in electrolyte medium may be effectively facilitated by adding nano-particles to the polymer electrolyte. The enhanced ion mobility of the nano-particles polymer electrolyte gel may be explained by an ion exchange mechanism with the formation of an electron transport path [65–68]. We have also measured the EIS spectra of the quasi-solid state DSSC under illumination at a bias voltage equal to open circuit voltage of the cells. It was observed that the impedance in low frequency range is significantly reduced by the nano-particles in the polymer electrolyte due to the improved ion mobility. The electron lifetime was calculated from the Bode plots of impedance spectra. The DSSC based on TiO_2–polymer electrolyte shows the longer electron lifetime mostly due to the reduction in dark current.

The IPCE curve of quasi-solid state DSSC (D3) is also shown in Fig. 7. The introduction of nano-filler induces a significant improvement in IPCE through out the whole wavelength region. The over all power conversion efficiency of the quasi-solid state DSSC with electrolyte containing TiO_2 nano-particles is about 3.2%. The enhancement in the solar cell performance upon the introduction of the TiO_2 nano-fillers in the polymer electrolyte is due to the improved ion conductivity and enhanced electron lifetime.

4. Conclusion

The modified TiO_2 photo-electrode was prepared for the fabrication of quasi-solid state dye sensitized solar cells based on polymer gel electrolyte, perylene derivative as sensitizer and PEDOT:PSS/graphite/FTO as counter electrode. The result indicates the increase of power conversion efficiency with the TiO_2 photo-electrode with compact TiO_2 layer inserted between FTO and np-TiO_2 layer, attributed to not only in the improvement of light harvesting property of the photo-electrode but also efficient electron transfer and reduced recombination. The compact TiO_2 film only provide a larger TiO_2/FTO contact area, but also effectively reduce the electron recombination by minimizing the direct contact between redox couple in electrolyte and conductive FTO surface. The addition of TiO_2 nano-particles in polymer electrolyte

further improve the power conversion efficiency (3.2%) attributed to the enhanced ion transport. It is expected that these finding will provide good insight into the design of quasi-solid state dye sensitized solar cells with efficient polymer gel electrolyte with nano-fillers.

Acknowledgement

References

[1] C.R. McNeil, J.J.M. Halls, R. Wilson, G.L. Wniting, S. Berkebite, M.C. Ramsey, R.H. Friend, N.C. Greenham, Adv. Funct. Mater. 18 (2008) 1.
[2] M.M. Mandoc, W. Veurman, L.J.A. Koster, B. deBoer, P.W.M. Blom, Adv. Funct. Mater. 17 (2008) 2167.
[3] G. Li, V. Shrotriya, J. Huang, Y. Yao, T. Moriarty, K. Emery, Y. Yang, Nat. Mater. 4 (2005) 864.
[4] C. Zhang, S.W. Tong, C. Jiang, E.T. Kang, D.S.H. Chen, C. Zhu, Appl. Phys. Lett. 92 (2008) 083310.
[5] J.Y. Kim, K. Lee, N.E. Coates, D. Moses, T.Q. Nguyen, M. Dante, Science 317 (2007) 222.
[6] J. Peet, Y.J. Kim, N.E. Coates, W.L. Ma, D. Moser, A.J. Heeger, G.C. Bazen, Nat. Mater. (2007).
[7] A.J. Moule, S. Allard, N.M. Kronenberg, A. Tsami, U. Scherf, K. Meerholz, J. Phys. Chem. C112 (2008) 12583.
[8] J.B. Boucle, S. Cryla, M.S.P. Shaffer, J.R. Durrant, D.D.C. Bradley, J. Nelson, Adv. Funct. Mater. 18 (2008) 622.
[9] Y.T. Lin, T.W. Zeng, W.Z. Lai, C.W. Chen, Y.Y. Lin, Y. Sheng, W.F. Su, Nanotechnology 17 (2006) 5781.
[10] D.C. Olson, S.E. Shaheen, R.T. Collins, D.S. Ginley, J. Phys. Chem. C111 (2007) 16670.
[11] B. O'Regan, M. Gratzel, Nature 353 (1991) 737.
[12] M.K. Nazeeruddin, P. Pechy, T. Renouard, S.M. Zakeeruddin, R. Humphry-Baker, P. Comte, P. Liska, P. Liska, L. Cevery, E. Costa, V. Shklover, L. Spiccia, G.B. Deacon, C.A. Bignozzi, M. Gratzel, J. Am. Chem. Soc. 123 (2001) 1613.
[13] M. Adachi, Y. Murata, J. Takao, J. Jiu, M. Sakamoto, F. Wang, J. Am. Chem. Soc. 126 (2004) 1613.
[14] N.G. Park, M.G. Kang, M.K. Kim, K.S. Ryu, S.H. Chang, J. van de Lagemaat, K.D. Benkstein, A.J. Frank, Langmuir 20 (2004) 4246.
[15] H.S. Lung, J.K. Lee, S. Lee, K.S. Hong, H. Shin, J. Phys. Chem. C112 (2008) 8476.
[16] D. Zhao, T. Peng, L. Lu, P. Cai, P. Jiang, Z. Bian, J. Phys. Chem. C 112 (2008) 8486.
[17] M. Gratzel, Nature 414 (2001) 338.
[18] M. Gratzel, J. Photochem. Photobiol. A164 (2004) 3.
[19] S. Yanagida, C.R. Chim. 9 (2006) 597.
[20] Z. Wang, Y. Cui, K. Hara, Adv. Mater. 19 (2007) 1.
[21] Y. Shibano, T. Umeyama, Y. Matano, H. Imahori, Org. Lett. 9 (2007) 1971.
[22] D. Kim, J.K. Lee, S.O. Kang, J. Ko, Tetrahedron 63 (2007) 1913.
[23] C.S. Karthikeyan, H. Wietasch, M. Thelakkat, Adv. Mater. 19 (2007) 1091.
[24] B. Pradhan, S.K. Batabyal, A.J. Pal, Sol. Energy Mater. Sol. Cells 91 (2007) 769.
[25] M.S. Roy, P. Balraju, M. Kumar, G.D. Sharma, Sol. Energy Mater. Sol. Cells 92 (2008) 909.
[26] X. Zhang, H. Yang, H.M. Xiong, F.Y. Li, Y.Y. Xia, J. Power Sources 160 (2006) 1451.
[27] M. Biancardo, K. West, F.C. Krebs, J. Photochem. Photobiol. A187 (2007) 395.
[28] H. Yang, M. Huang, J. Wu, Z. Lan, S. Hao, J. Lin, Mater. Chem. Phys. 110 (2008) 38.
[29] A.F. Nogueira, J.R. Durrant, M.A. De Paoli, Adv. Mater. 13 (2001) 826.
[30] T. Stergiopoulos, I.M. Arabatzis, G. Katsaros, P. Falaras, Nano Lett. 2 (2002) 1259.
[31] G. Nazmutdinova, S. Senfuss, M. Schrodner, A. Hinsch, R. Sastrawan, D. Gerhard, S. Himmler, P. Wasserschrid, Solid State Ionics 177 (2006) 3141.
[32] S. Ito, P. Liska, P. Comte, R. Charvet, P. Pechy, U. Boch, L. Schmidt-Mende, S.M. Zakeeruddion, A. Kay, M.K. Nazeeruddin, M. Gratzel, Chem. Commun. (2005) 4351.
[33] B. Peng, G. Jugmnn, C. Jager, D. Haarer, H.W. Schmidth, M. Jhelakkat, Coord. Chem. Rev. 248 (2001) 1479.
[34] H. Tributsch, Appl. Phys. A: Mater. Sci. Process. 73 (2001) 305.
[35] P.J. Cameron, L.M. Peter, J. Phys. Chem. B 107 (2003) 14394.
[36] M. Durr, A. Yasuda, G. Nelles, Appl. Phys. Lett. 89 (2006) 061110.
[37] H. Nusbaumer, J.E. Moser, S.M. Zakeeruddion, M.K. Nazeeruddin, M. Gratzel, J. Phys. Chem. B 105 (2001) 10461.
[38] J. Kruger, R. Piass, L. Ceuey, M. Piccirelli, M. Gratzel, Appl. Phys. Lett. 79 (2001) 2085.
[39] R. Hattari, H. Goto, Thin Solid Films 515 (2007) 8045.
[40] P.K. Song, Y. Irie, S. Ohno, Y. Sato, Y. Shigesoto, Jpn. J. Appl. Phys. 43 (2004) L442.
[41] S. Ohno, D. Sato, M. Kon, M. Yoshikanto, K. Suzuki, P. Frach, Y. Shigesato, Thin Solid Films 445 (2003) 207.
[42] Y. Shibata, T. Kato, T. Kado, R. Shiratuchi, W. Takashima, K. Kaneto, S. Hayase, Chem. Commun. (2003) 2730.
[43] Y. Satio, W. Kubo, T. Kitamura, Y. Wada, S. Yanagida, J. Photochem. Photobiol. A 164 (2004) 153.
[44] M. Biancardo, K. West, F.C. Krebs, J. Photochem. Photobiol. A 187 (2007) 395.
[45] C. Zafer, M. Kus, G. Turkmen, H. Dincalp, S. Demic, B. Kuban, Y. Teoman, S. Icli, Sol. Energy Mater. Sol. Cell 91 (2007) 427–431.
[46] H. Tian, P.-H. Liu, W. Zhu, E. Gao, D.-J. Wu, S. Cai, J. Mater. Chem. 10 (2000) 2708–2715.
[47] B.A. Gregg, S. Ferrere, New J. Chem. 26 (2002) 1155–1160.
[48] Y. Shibano, T. Umeyama, Y. Matano, H. Imahori, Org. Lett. 9 (2007) 1971–1974.
[49] Jĭ. Fortage, M. Sĭeverac, C. Houarner-Rassin, Y. Pellegrin, E. Blart, F. Odobel, J. Photochem. Photobiol.: Chem. 197 (2008) 156–169.
[50] A. Hagfeldt, M. Gratzel, Chem. Rev. 95 (1995) 49.
[51] P.V. Kamat, S. Das, K.G. Thomas, M.V. George, Chem. Phys. Lett. 178 (1991) 75.
[52] C. Karapire, C. Zafer, S. Icli, Synth. Met. 145 (2004) 51.
[53] B. Burfeindt, T. Hannappel, W. Storck, F. Willig, J. Phys. Chem. 100 (1996) 16463.
[54] T. Hannappel, B. Burfeindt, W. Storck, F. Willig, J. Phys. Chem. 101B (1997) 6799.
[55] S. Ferrere, A. Zaban, B.A. Gregg, J. Phys. Chem. B 101 (1997) 4490.
[56] J.Y. Kim, I.J. Chung, J.K. Kim, J.W. Yu, Curr. Appl. Phys. 6 (2006) 969–973.
[57] S. Wang, Y. Li, C. Du, Z. Shi, S. Xiao, D. Zhua, E. Gao, S. Cai, Synth. Met. 128 (2002) 299–304.
[58] B.C. O'Regan, J.R. Durrant, P.M. Sommeling, N.J. Bakker, J. Phys. Chem. C111 (2007) 14001.
[59] A.N.M. Green, E. Palomares, S.A. Haque, J.M. Kroon, J.R. Durrant, J. Phys. Chem. B109 (2005) 4616.
[60] J. Bisquert, A. Zuban, M. Greenshtein, I. Mora-Sero, J. Am. Chem. Soc. 126 (2004) 13550.
[61] A. Zuban, M. Greenshtein, J. Bisquert, Chem. Phys. Chem. 4 (2003) 859.
[62] J. Bisquert, J. Phys. Chem. B106 (2002) 325.
[63] Q. Wang, J.E. Moser, M. Gratzel, J. Phys. Chem. B106 (2002) 325.
[64] R. Kern, R. Sastrawan, J. Ferber, R. Stangel, J. Luther, Electrochim. Acta 47 (2002) 4213.
[65] T. Hoshikawa, M. Yamada, R. Kikuchi, E. Eguchi, J. Electrochem. Soc. 152 (2005) E68.
[66] M. Adachi, M. Sakamoto, J. Jiu, Y. Ogata, S. Isuda, J. Phys. Chem. B 110 (2006) 13872.
[67] H. Usual, H. Matsui, N. Tanabe, S. Yanagida, J. Photochem. Photobiol. A: Chem. 164 (2004) 97.
[68] M.S. Kang, K.S. Ahn, J.W. Lee, J. Power Sources 180 (2008) 896.